Electronic Supplementary Material (ESI) for Nanoscale.
This journal is © The Royal Society of Chemistry 2021

Supporting Information

Improved zT in Nb_5Ge_3 - GeTe Thermoelectric Nanocomposite

Jing Cao[a], Xian Yi Tan[a,b], Ning Jia[b], Da Lan[c], Solco Samantha Faye Duran[a], Kewei Chen[d], Sheau Wei Chien[a], Hongfei Liu[a], Chee Kiang Ivan Tan[a], Qiang Zhu[a], Jianwei Xu[a], Qingyu Yan[b], Ady Suwardi[a,c*]

[a] Institute of Materials Research and Engineering, #08-03, 2 Fusionopolis Way, Agency for Science, Technology and Research, Singapore 138634.

[b] School of Materials Science and Engineering, Nanyang Technological University, Singapore 639798.

[c] Department of Materials Science and Engineering, National University of Singapore, Singapore 117575.

[d] School of Mechanical and Aerospace Engineering, Nanyang Technological University, Singapore 639798.

Corresponding: ady_suwardi@imre.a-star.edu.sg

Table S1. Physical properties used to model κ_L in GeTe based on various phonon scattering processes.

Parameters	Values
vL, m/s	3410
vT, m/s	1995
vm, m/s	2210
Atomic mass, kg	1.66×10^{25}
Sample density, g/cm3	6.14
Debye T, K	122
γ	1.45
Poisson's ratio	0.24
Bulk modulus, GPa	39.9
Young's Modulus, GPa	62.2
Shear Modulus, GPa	25.5
Grain size, um	42

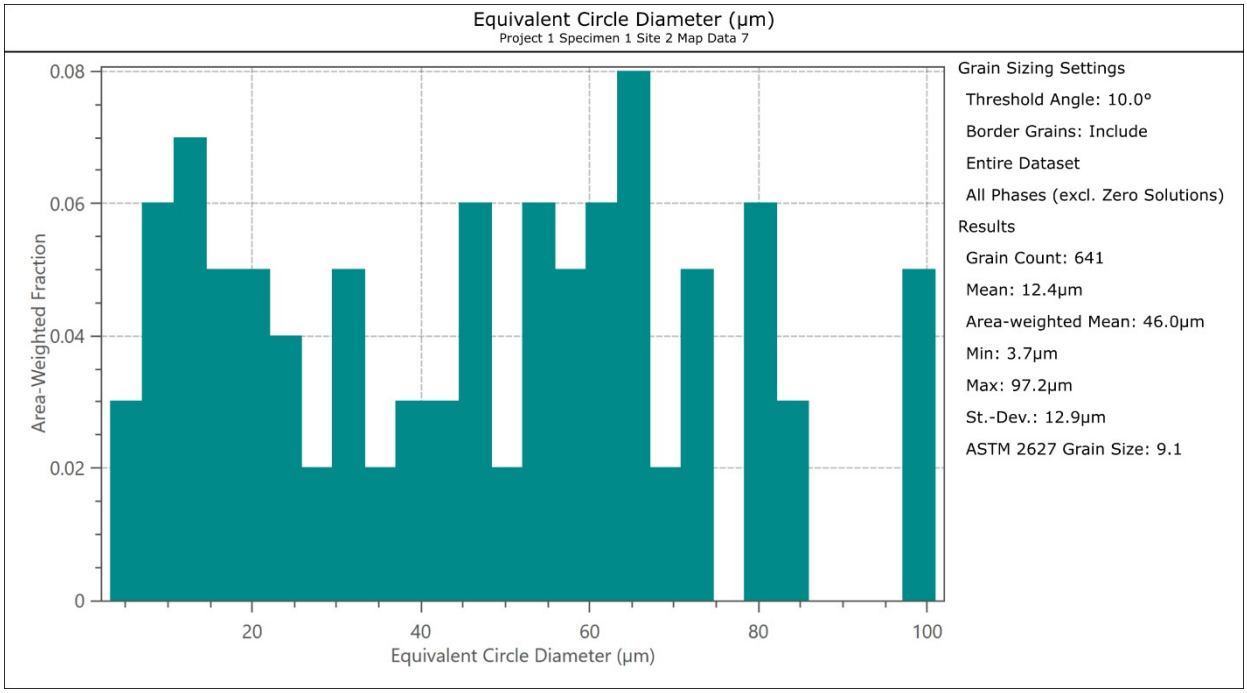

Figure S1. Grain size distribution of EBSD mapping.

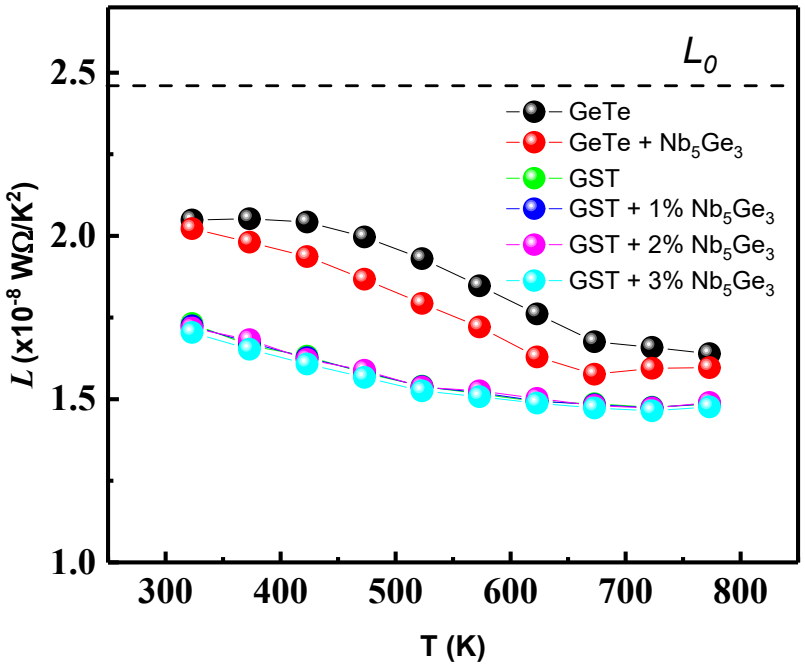

Figure S2. Lorenz number from Single Parabolic Band for all samples

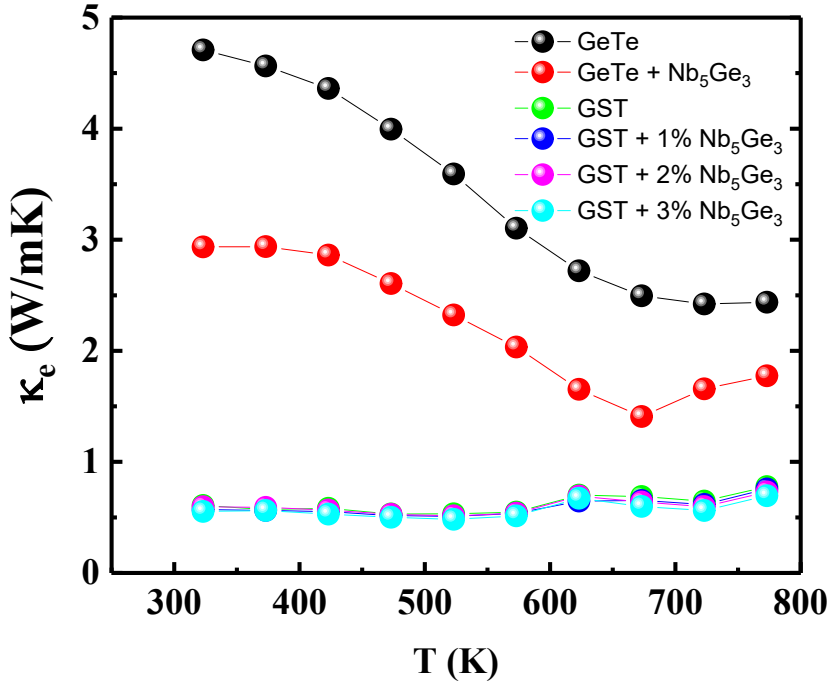

Figure S3. Electronic thermal conductivity for all samples

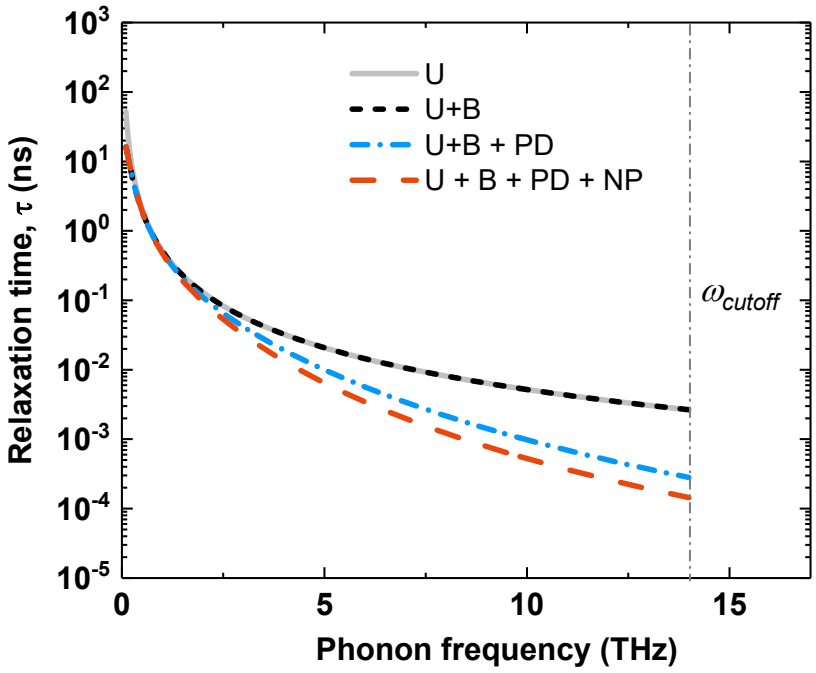

Figure S4. Phonon relaxation time as a function of frequency for various scattering processes.

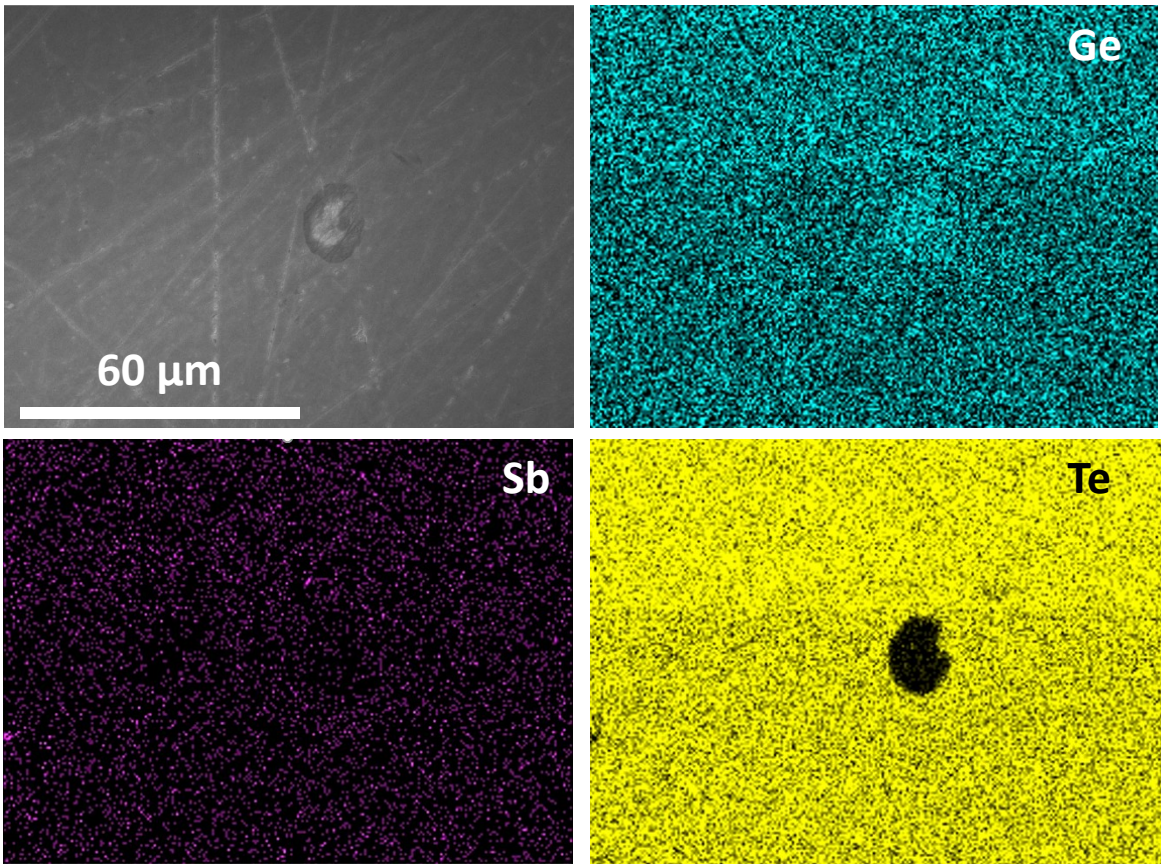

Figure S5. SEM EDS of $Ge_{0.9}Sb_{0.1}Te$.

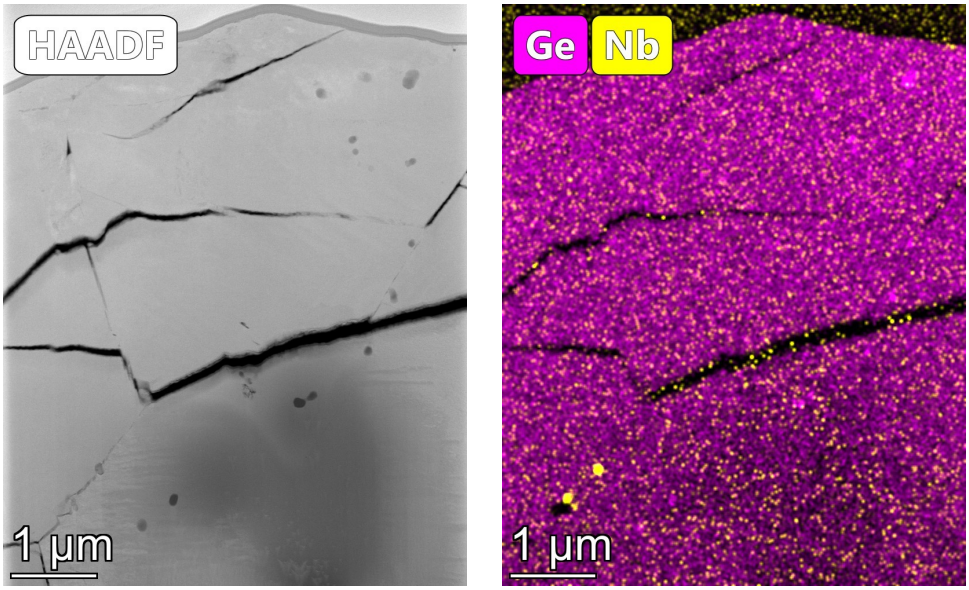

Figure S6. TEM HAADF (High angle annular dark field) image and the corresponding EDS showing finely (nm sized) dispersed regions of Nb_5Ge_3 in the GeTe-Nb_5Ge_3 doped sample.

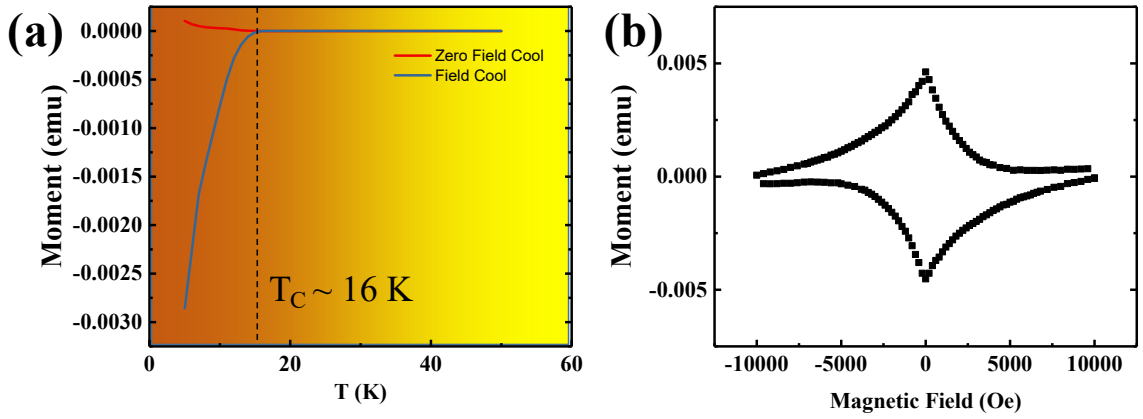

Figure S7. (a) Temperature dependence of magnetization for both zero field cooled and field cooled processes. (b) Magnetization hysteresis measured at superconducting state (5 K).

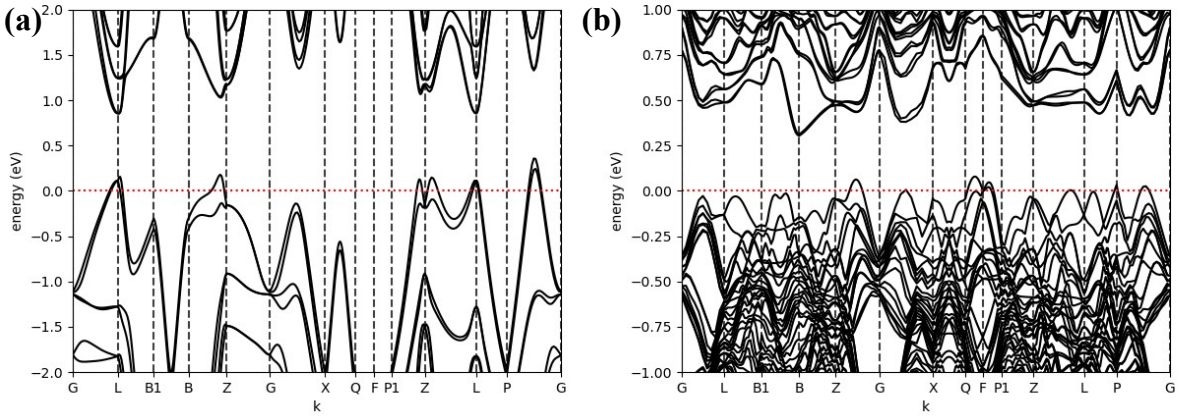

Figure S8. (a) Electronic band structure of rhombohedral GeTe and (b) cubic $Ge_{0.9}Sb_{0.1}Te$.

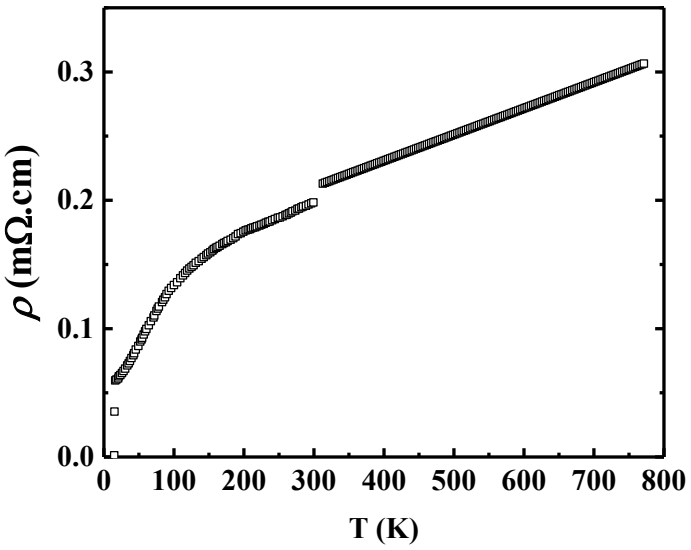

Figure S9. Resistivity vs temperature data for Nb_5Ge_3.

Weighted Mobility μ_W

To understand the nature of transport in more detail, we compute the σ_{E_0} from electrical conductivity σ, which can be expressed as:

$$\sigma = \sigma_{E_0} \ln (1 + e^{\eta}) \tag{1}$$

Essentially, $\sigma_{E_0}$is a convenient expression of electrical conductivity that is independent of carrier concentration. This is especially useful in our case since the carrier concentration values obtained via Hall measurements may not be accurate due to the non-linearity of the Hall voltage versus magnetic field. (i.e. the Hall carrier concentration is typically taken as the linear slope of Hall voltage versus magnetic field, non-linearity in Hall voltage versus magnetic field makes data interpretation inaccurate). Large σ_{E_0} can be associated with good crystalline quality and vice versa. Furthermore, the carrier mobility-equivalent for σ_{E_0} can be expressed as weighted-mobility μ_W. The relation between σ_{E_0} and μ_W can be expressed as:

$$\sigma_{E_0} = \frac{e(2m_e k_B T)^{3/2}}{3\pi^2 \hbar^3} \mu_W \quad (2)$$

$$\mu_W = \mu_0 \left(\frac{m_{DOS}^*}{m_e}\right)^{3/2} \quad (3)$$

The main advantage of using weighted-mobility over inaccurately determined Hall mobility lies in the fact that weighted-mobility takes into account the m_{DOS}^* (density of states effective mass). Since the density of states effective mass provides a direct correlation to the Seebeck coefficient, the inverse correlation between electrical conductivity and Seebeck coefficient can be clearly accounted for by looking at the weighted mobility. Hence, it can be used as a robust indication of the thermoelectric power factor. It is important to note that while weighted mobility share some similarities with Hall mobility, their magnitude generally differs, especially for compounds with high band-degeneracy (high m_{DOS}^*). This comes from the fact that weighted mobility has a $m_{DOS}^{*3/2}$ dependence whereas Hall mobility only depends on μ_0(intrinsic mobility) as well as the reduced Fermi level and scattering mechanism.

Lastly, the quality factor B can be evaluated from σ_{E_0} based on the following:

$$B = \left(\frac{k_B}{e}\right)^2 \frac{T}{k_L} \sigma_{E_0} \quad (4)$$

It is evident from equation 5 that in order to enhance the quality factor, σ_{E_0} must be enhanced, either via band convergence, resonant doping, energy filtering, or deformation potential engineering to increase m_{DOS}^*. Alternatively, k_L can be reduced via point defects, strain, dislocation, or stacking faults.

Lorenz Number

The Lorenz number used in this work is calculated from the semiclassical Boltzmann Transport Equations under single parabolic band assumption:

$$L = \left(\frac{k_B}{e}\right)^2 \left[\frac{\left(r + \frac{7}{2}\right)F_{r+1.5}(\eta)}{\left(r + \frac{3}{2}\right)F_{r+0.5}(\eta)} - \left(\frac{\left(r + \frac{5}{2}\right)F_{r+1.5}(\eta)}{\left(r + \frac{3}{2}\right)F_{r+0.5}(\eta)}\right)^2\right] \quad (5)$$

Where *r* represents the carrier scattering exponent, set at -0.5 for acoustic phonon scattering.

Simplified Debye-Callaway model for lattice thermal conductivity

In order to model the lattice thermal conductivity, Debye frequency was first determined from:

$$\omega_{max} = \omega_D = \left(\frac{6\pi^2}{V}\right)^{1/3} v_m \quad (6)$$

Where V is the atomic volume and v_m was obtained from equation (4). The acoustic branch maximum frequency can be expressed as:

$$\omega_a = \frac{\omega_D}{N^{1/3}} \quad (7)$$

Where N is the number of atoms per unit cell.

The Debye temperature θ_D can then be expressed as:

$$\hbar\omega_D = k_B\theta_D \tag{8}$$

Subsequently, the phonon relaxation time *τ(ω)* can be calculated by accounting for contribution from Umklapp, grain boundaries, and point defects as following:

$$\tau_U^{-1} = \frac{2}{(6\pi^2)^{1/3}} \frac{k_B V^{1/3} \gamma^2 \omega^2 T}{\bar{M} v^3} \tag{9}$$

$$\tau_B^{-1} = \frac{v}{d} \tag{10}$$

$$\tau_{PD}^{-1} = \frac{V\omega^4}{4\pi v^3} \left(\sum_i f_i \left(1 - \frac{m_i}{\bar{m}}\right)^2 + \sum_i f_i \left(1 - \frac{r_i}{\bar{r}}\right)^2 \right) \tag{11}$$

In our case, the spectral heat capacity $C_s(\omega)$ can be expressed as:

$$C_s(\omega) = \frac{3k_B\omega^2}{2\pi^2 v^3} \tag{12}$$

By assuming constant group velocity (sound velocity), we can express the spectral thermal conductivity $\kappa_s(\omega)$ as:

$$\kappa_s(\omega) = C_s(\omega) v^2 \tau(\omega) \tag{13}$$

Finally, the lattice thermal conductivity can be obtained by integrating the spectral thermal conductivity over the entire frequency range up to ω_a:

$$\kappa_L = \frac{1}{3} \int_0^{\omega_{max}} C_s(\omega) v^2 \tau(\omega) d\omega \tag{14}$$

In our experiments, we obtained both **elastic constant (*E*)** from nanoindentation as well as **longitudinal sound velocity (v_L)** from ultrasonic measurements. In order to obtain other elastic properties, we made use of the following equations:

$$B = \frac{E}{3(1 - 2v_p)} \tag{15}$$

Where B = Bulk modulus; v_p = Poisson ratio

Both sides of the above equation can be expressed in terms of v_L and v_T (longitudinal and transverse sound velocity, respectively) as follows:

$$B = \rho\left(v_L^2 - \frac{4}{3}v_T^2\right) \tag{16}$$

$$v_p = \frac{1 - 2(\frac{v_T}{v_L})^2}{2 - 2(\frac{v_T}{v_L})^2} \tag{17}$$

Where ρ = density

The transverse sound velocity v_T can then be calculated by substituting equation (2) and (3) into equation (1) and solving for v_T. Subsequently, the average sound velocity, v_m can be determined via:

$$v_m = \left(\frac{1}{3}\left[\frac{1}{v_L^3} + \frac{2}{v_T^3}\right]\right)^{-\frac{1}{3}} \tag{18}$$

Shear modulus μ can be obtained from:

$$\mu = \rho v_T^2 \tag{19}$$

In addition, after obtaining the poisson ratio v_p from equation (3), the Gruneisen parameter γ can be determined by:

$$\gamma = \frac{3}{2}\left(\frac{1 + v_p}{2 - 3v_p}\right) \tag{20}$$

Hall Concentration and Mobility

Table S2. Hall concentration and Hall mobility of all samples.

Composition	n_H **(cm^{-3})**	μ_H **(cm^2/Vs)**
GeTe	8.1 x 10^{20}	55.1
GeTe – 0.5% Nb_5Ge_3	7.5 x 10^{20}	38.0
$Ge_{0.90}Sb_{0.10}Te$	1.9 x 10^{20}	33.9
$Ge_{0.90}Sb_{0.10}Te$ – 1 % Nb_5Ge_3	1.7 x 10^{20}	38.1
$Ge_{0.90}Sb_{0.10}Te$ – 2 % Nb_5Ge_3	2.0 x 10^{20}	34.2
$Ge_{0.90}Sb_{0.10}Te$ – 3 % Nb_5Ge_3	1.9 x 10^{20}	28.7

Table S3. Lattice parameters of Pristine GeTe compared to doped samples. No drastic change in lattice parameters can be observed.

Composition	***a*** **(Å)**	***b*** **(Å)**	***c*** **(Å)**	α	β	γ
GeTe	4.17 ± 0.00009	4.17 ± 0.00009	10.65 ± 0.00026	90	90	120
GeTe – 0.5% Nb_5Ge_3	4.17 ± 0.00012	4.17 ± 0.00012	10.66 ± 0.00033	90	90	120
$Ge_{0.90}Sb_{0.10}Te$	4.19 ± 0.00017	4.19 ± 0.00017	10.41 ± 0.00046	90	90	120
$Ge_{0.90}Sb_{0.10}Te$ – 1 % Nb_5Ge_3	4.19 ± 0.00014	4.17 ± 0.00014	10.44 ± 0.00031	90	90	120

$Ge_{0.90}Sb_{0.10}Te$ – 2 % Nb_5Ge_3	4.18 ± 0.00011	4.18 ± 0.00011	10.46 ± 0.00027	90	90	120
$Ge_{0.90}Sb_{0.10}Te$ – 3 % Nb_5Ge_3	4.17 ± 0.00012	4.17 ± 0.00012	10.41 ± 0.00038	90	90	120